IDŐJÁRÁS

Quarterly Journal of the Hungarian Meteorological Service
Vol. 111, No. 1, January–March 2007, pp. 41–63

The Constitution Day storm in Budapest: Case study of the August 20, 2006 severe storm

Ákos Horváth[1*], **István Geresdi**[2], **Péter Németh**[3] and **Ferenc Dombai**[3]

[1]*Hungarian Meteorological Service, Storm Warning Observatory,*
Vitorlás u. 17, H-8600 Siófok, Hungary; E-mail: horvath.a@met.hu

[2]*University of Pécs, Institute of Environmental Sciences,*
Ifjúság u. 6, H-7624 Pécs, Hungary; E-mail: geresdi@gamma.ttk.pte.hu

[3]*Hungarian Meteorological Service,*
P.O. Box 39, H-1675 Budapest, Hungary;
E-mails: nemeth.p@met.hu; dombai.f@met.hu

(Manuscript received in final form March 5, 2007)

Abstract—In the evening of August 20, 2006 severe thunderstorms hit Budapest. The storm struck the downtown at the same time when the Constitution Day firework just started, killed five people and wounded hundreds of spectators crowded on the embankments of the river Danube. In this paper weather conditions from synoptic scale to storm scale are investigated to find the special circumstances, which led to formation of the devastating storm. Investigations show that a wave on a cold front, the mid level cold advection, the drift of jet stream above the warm sector, and an intense wet conveyor belt resulted in intense instability. Furthermore, the wind shear and the low level convergence also contributed to the formation of the fast moving squall line. Detailed Doppler-radar analysis proved that the thunderstorm, which crossed the downtown of Budapest, was a supercell. Comparison of the radar reflectivity and the lightning data of the investigated case with that of other severe storm cases shows that the Constitution Day storm was not an extreme event. The unique feature of this case was the extreme high speed of cell motions. High resolution numerical model (MM5) was applied to understand the dynamical structure and predictability of the storm. Model results show the importance of the layer on 3 km above ground level with high value of equivalent potential temperature and the active role of the cold front in the formation of the squall line. The model was able to simulate the structure and motion of the supercell proving the numerical predictability of this type of severe convective storms.

Key-words: squall line, supercell, MM5, severe convective storm, Doppler-radar

[*] Corresponding author

1. Introduction

Late afternoon on August 20, 2006, a squall line coming from the north-west direction reached the western border of Hungary. Surface and radar observations showed, that thunderstorm cells moved fast and some of them were extremely intensive. The north part of the squall line arrived in Budapest at 19:00 UTC, when the traditional Constitution Day's firework had just started. In the centre of Budapest, more than half million people crowded on the embankments and bridges of the river, and numerous spectators watched the event from boots drifting on the Danube, too. The thunderstorm produced wind gusts reached 32.3 m/s in the centre of downtown (measured on the top of the building of the Hungarian Meteorological Service), and 34.1 m/s in the southern part of the downtown (measured on the top of the building of the University of Science). Broken trees and fragments from roof of houses hit into crowds causing injuries and panic. Five people were killed and hundreds were injured due to the extreme weather. The strong wind caused a loss of about 5 million USD in buildings and cars.

Severe thunderstorms and associated phenomena like stormy wind gusts, hailstorms, heavy rainfalls, sometimes tornadoes often occur in Hungary, especially in summer. The facts presented in this paper suggest that this storm was a supercell thunderstorm, one of the types of severe convective phenomena which are observed from time to time in Hungary (*Horváth* and *Geresdi*, 2003). Structure and development of severe convective phenomena have been investigated since the beginning of the 1950's. Among others, pioneering work of Fujita described the phenomenology of squall lines (*Fujita*, 1955), and the origin of thunderstorm pressure-heights (*Fujita et al*., 1959). Meteorological satellites and radars have become the main tools for investigation and operative forecast of severe convection (*Reyonolds et al*., 1979). These remote sensing equipments and the surface meso-networking observations allowed to develop comprehensive theories of the mesoscale convective system (MCS) such as long-lived squall lines (*Rotunno et al*., 1988; *Houze et al*., 1989). The most devastating mesoscale phenomena are the supercells which are mostly associated with MCS. The presently accepted theory about the dynamics and necessary conditions of supercell formation was published by *Klemp* (1987). Most of the MCSs and supercells form in the unstable region of cyclones and frontal systems. Prefrontal conditions – large convective available potential energy, horizontal and vertical wind shears (*Davies-Jones et al*., 2001) – can produce favorable environment for the supercell formation. The convergence and vertical circulation of frontal system (*Hoskins*, 1972) also promote the MCS formation, especially if the MCS is connected with the circulation of the jet stream (*Shapiro*, 1982).

The first numerical experiments about the simulation of convective storms used twodimensional models in the 1960's (*Lilly*, 1962). The large computer capacity necessary for the three-dimensional simulation of thunderstorms (e.g., *Klemp*, 1978) was available by the late 70's. Supercells and squall lines are very complex atmospheric phenomena, so they can be simulated only with state-of art numerical models which involves non-hydrostatic version of equation of motion, detailed description of short and long wave radiation, processes occuring in the boundary layer, and formation of precipitation and cloud elements (*Wilhelmson*, 2001).

Early investigations of severe thunderstorms in Hungary were motivated by improving the efficiency of the storm warning at Lake Balaton (*Götz*, 1966; *Böjti et al*., 1964; *Götz*, 1968). The hail suppressing system operated in the 1980's required the investigation of microphysical processes occuring in thunderstorms (*Zoltán* and *Geresdi*, 1984). Dynamical conditions of the formation of squall lines in the Carpathian Basin were investigated by *Horváth* and *Práger* (1985). *Bartha* (1987) worked out an empirical method to predict maximum wind gusts of thunderstorm cells. *Bodolainé* and *Tänczer* (2003) investigated flash flood causing mesoscale convective complexes in the Carpathian Basin. The nowcasting system of the Hungarian Meteorological Service gave a new tool for the ultrashort term forecast of severe weather (*Geresdi* and *Horváth*, 2000; *Horváth* and *Geresdi*, 2003; *Geresdi et al*., 2004). Appearances of supercells and formation of tornadoes in Hungary was described first time by *Horváth* (1997). Due to the increased authenticity of radar in the weather radar network of Hungarian Meteorological Service (HMS) by the end of the 90's, more supercell cases were recognized (*Horváth*, 1997; *Horváth* and *Geresdi*, 2003). Not only the observation background has been improved, but a new tool for the numerical simulation of supercells and tornadoes became available by using limited area non-hydrostatic model MM5 (*Horváth et al*., 2006).

In the first section of the paper the synoptic scale conditions of formation and development of the Budapest storm are shown by using ECMWF analysis and forecast. In the second section the development, movement, and other characteristics of the storm cells are analyzed by using radar data. In the third section results of MM5 model with high resolution are discussed. The general and special features, furthermore, the predictability of the Budapest storm are given in the conclusion.

2. Synoptic scale weather conditions

On August 20, 2006 a long and thermally sharp cold front crossed Central and Southern Europe moving to the east. On the 850 hPa pressure level the temperature difference between the warm sector and the postfrontal region was 10–12 °C. In the southern part of the long frontal system, between 00:00 and

12:00 UTC, a frontal wave developed. This wave – behaving like a temporary warm front – expanded to the Alps by 15:00 UTC (*Fig. 1*). The dotted line in *Fig. 1* represents the leading edge of a weak high level cold airmass, which moved above the warm sector. Signs of this high level cold advection can be seen in the figure of 500 hPa temperature and wind fields (*Fig. 2*). The high level cold air could move there, because the low level wave of the long cold frontal system did not affect upper streams, and they continued their drifting toward the east. In the cross section of potential vorticity field a positive local maximum can also be associated with the mid tropospheric cold advection (*Fig. 3*). The second important feature of the weather pattern is the extremely intense wet conveyor belt at the 700 hPa level (*Fig. 4*). In the layer of the wet conveyor belt the maximum values of relative humidity coincided with the significant wind maximum, which could be considered as the low level jet stream. The third characteristic is the upper level jet stream at the 300 hPa level (*Fig. 5*). The upper level strong wind results in vertical wind shear necessary for the formation of severe convective storm (*Holton*, 2004).

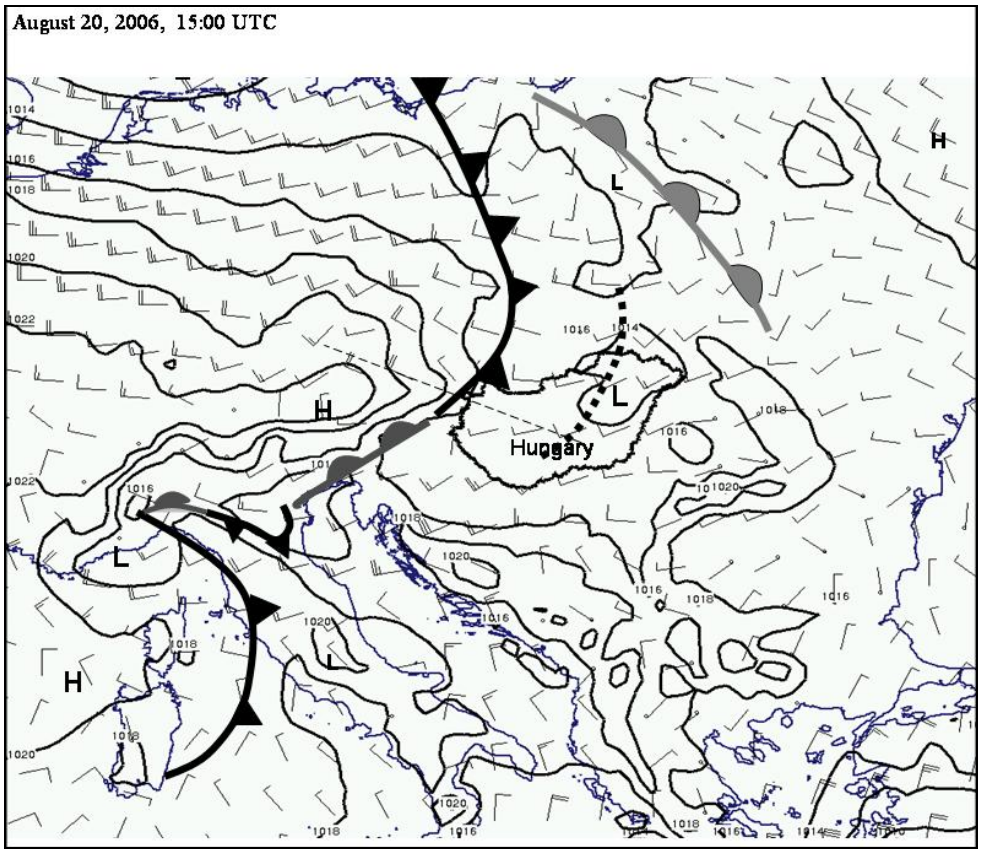

Fig. 1. ECMWF forecast of sea level pressure, 925 hPa wind, and fronts on August 20, 2006, 15:00 UTC. Dashed line shows the position of the direction of cross-section in Figs. 3 and 6.

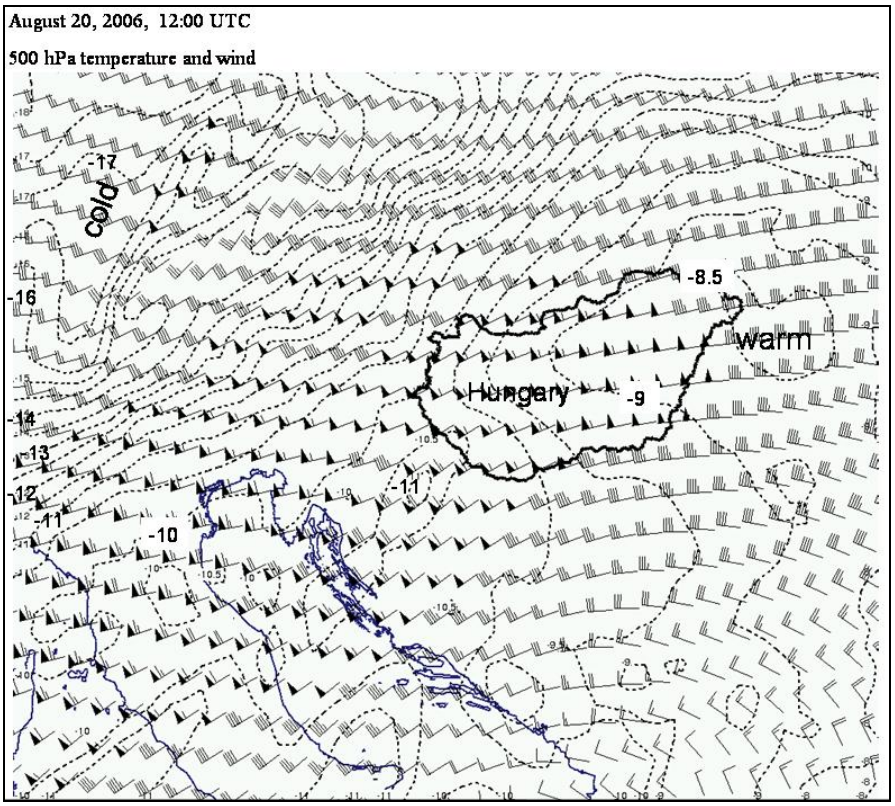

Fig. 2. 500 hPa wind and temperature (difference between the temperature isolines is 0.5 °C) on August 20, 2006, 12:00 UTC from the ECMWF analysis.

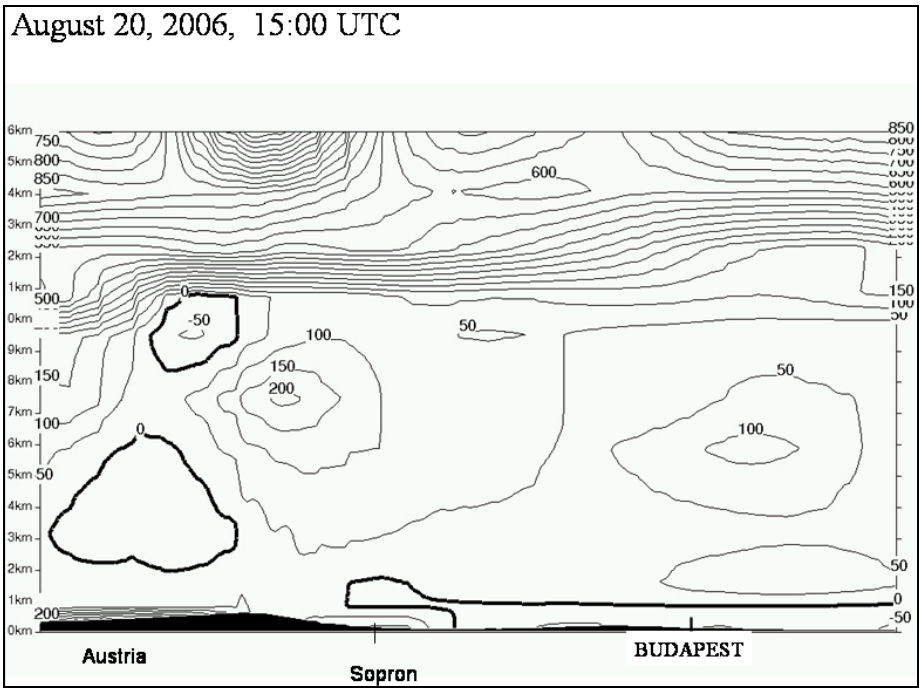

Fig. 3. Cross section of potential vorticity (10^{-5} s^{-1}) on August 20, 2006, 15:00 UTC from the ECMWF forecast. The direction of cross-section is denoted by dashed line in Fig. 1.

Fig. 4. 700 hPa wind and relative humidity on August 20, 2006, 12:00 UTC from the ECMWF analysis.

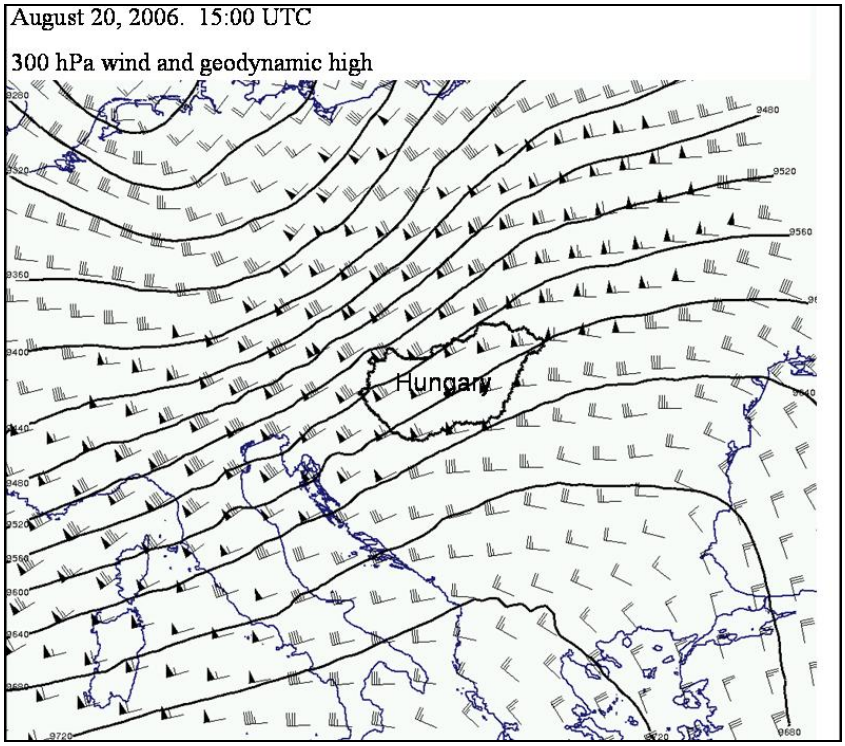

Fig. 5. 300 hPa wind and geopotentials on August 20, 2006, 15:00 UTC from the ECMWF forecast.

The direct role of the cold front in the formation of the Budapest storm is not obvious. Analysis of the ECMWF 12:00 UTC+6-hour forecast shows that the frontal system would not have reached Budapest by 19:00 UTC. The cross sections of potential vorticity and omega fields depict that the cold front reached the Hungarian border only at 18:00 UTC (*Fig. 6*). However observations show that the squall line was close to Budapest by this time.

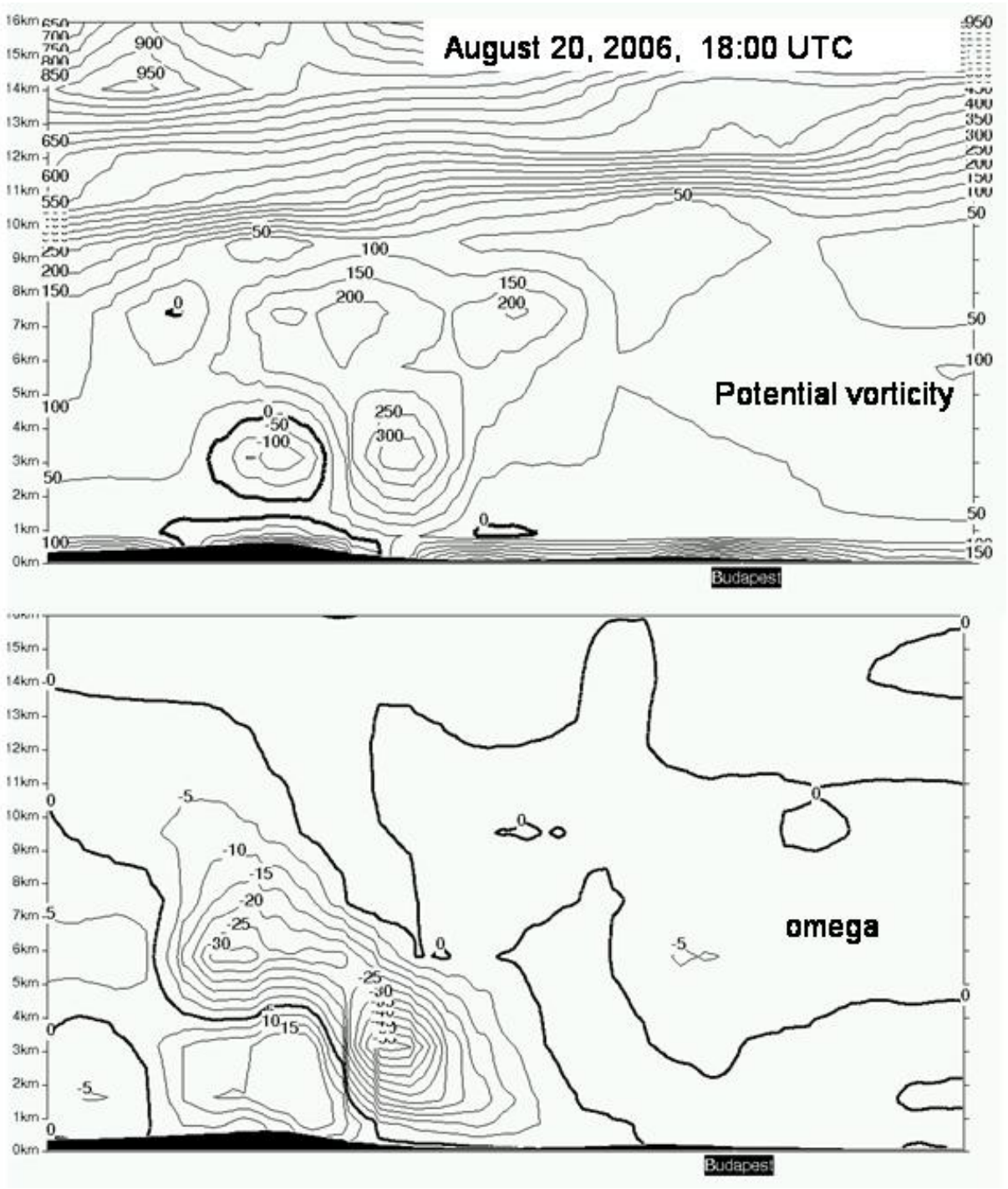

Fig. 6. Cross-section of potential vorticity (10^{-5} s^{-1}) and omega (10 Pa/h) at 18:00 UTC from the ECMWF forecast.

A possible explanation of the fact that thunderstorms arrived in Budapest 2 hours earlier than the modeled cold front is that a squall line separated from the front and run ahead. Because ECMWF forecast system is not suited for the simulation of convective scale processes, it was not able to predict the squall line. However it is notable that weather analysis could not distinguished different squall line and cold front in the time of Budapest storm.

Summing up the synoptic scale weather pattern in the investigated case one can state: (i) The wave of a sharp cold front formed an unstable warm sector, in which an intensive wet conveyor belt and strong high level jet stream resulted in favorable conditions for the formation of severe thunderstorms. (ii) After 15:00 UTC the effect of mesoscale convective processes became more dominant than that of the synoptic scale systems.

3. Observation of the Budapest storm

The HMS radar network detected the first significant radar echoes (R>40 dBZ) at the eastern part of the Alps at 13:00 UTC. The line structure of the position of the thunderstorms could be observed at 13:45 UTC, still in Austria. The squall line reached the Hungarian-Austrian border at 16:30 UTC (*Fig. 7a*). This time the observed wind gusts were below 20 m/s. At 17:45 UTC three main thunderstorm systems could be distinguished along the squall line: the first one was in the northern part, the second was in the center, and the third was in the southern part (*Fig. 7b*). Some of the weather stations reached by the squall line reported 22 m/s wind gusts at this time. By 18:15 UTC the most intensive thunderstorms appeared in the north part of the squall line, the maximum reflectivity was near 55 dBZ in this region. The thunderstorms in the central region became weaker, and the thunderstorms in the southern region fell behind the squall line (*Fig. 7c*). By 19:00 UTC the thunderstorms in the northerly part remained active, and their reflectivity maximum was near 60 dBZ (*Fig. 7d*). The north part of the squall line reached Budapest when the thunderstorms were very intensive in it. Time series of radar images show that three of thunderstorm-centers have long-lived (>2 hours) comma like cells, and presumably these cells were supercells. The presence of the wall cloud in the photograph of Budapest storm shows some similarity to the supercell features. The maximum observed wind gust in Budapest was 34.1 m/s, but extent of damage suggests even higher maximum wind speeds. An eyewitness reported funnel cloud, but it was not confirmed. The thunderstorm system moved to southeast direction, and at about 30 km southeast of Budapest a 38.3 m/s wind gust was measured. After leaving Budapest the system remained active as long as it reached the line of the river Tisza.

Fig. 7. Position of the squall line given by radar reflectivity.

3.1 Radar and lightening data

Thunderstorm formation and development were observed by the DWSR 2500 radar based weather radar network (3 radars) and SAFIR 3000 (7 sensors) based lightning location network of HMS. The data of these measurements were available in real time on the synoptic workstation of HMS all day. The basic radar and lightning characteristics were derived from the data of the routine observation, which include the national radar composites of CMAX dBZ values (maximum dBZ from 9 different elevations in every column) over a 800 km × 500 km region. The radar pictures were completed in every 15th minutes. The lightning events were recorded continuously this day providing data on IC and CG flashes. In our investigation these two data sets were carefully aligned in space and time. A site error compensation method was applied to reduce the large location errors of SAFIR system.

The radar and lightning data of the thunderstorms developed on August 20, 2006 did not show any unique or extreme characteristics. More intensive thunderstorms were observed on 7 days in this year. The total amount of flashes

and precipitable water produced by the thunderstorms on August 20 can be considered as typical summer values in Hungary.

The main characteristics are summarized in *Table 1* for lightning data (comparing to an extreme active lightning day) and *Table 2* for radar data.

Table 1. General lightning characteristics for August 3, 2005 (an extreme active day) and August 20, 2006

Date	**Daily total**			**Maximum (15 min)**		
	Localization	**IC Flash**	**CG Flash**	**Density** $km^{-2}\ h^{-1}$	**Area** km^2	**Flashes**
08.03.2005	532,375	242,301	40,405	34.5	17,552	28,808
08.20.2006	28,270	14,580	964	7.5	3656	3170
Ratio	**18.8**	**16.6**	**41.9**	**4.6**	**4.8**	**9.1**

Table 2. General radar characteristics on August 3, 2005 and on August 20, 2006

Date	**Daily total**			**Maximum (15 min)**			
	Water million m^3 **>15 dBZ**	**Water million** m^3 **>45 dBZ**	**Mean rain >15 dBZ**	**dBZ**	**Area** km^2 **>15 dBZ**	**Water million** m^3 **>15 dBZ**	**Water million** m^3 **>45 dBZ**
08.03.2005	2040,14	44,76	1.83	57.0	98,924	350,0	28,0
08.20.2006	915,88	112,06	2.97	59.5	38,940	15,0	33,0
Ratio	**2.2**	**0.4**	**0.6**	**–2.5**	**2.5**	**2.3**	**0.8**

Computer programs were developed to calculate different kind of characteristics of thunderstorm cells from radar and lightning data. These codes provide minimum and maximum values of dBZ, area and center points of the cells, as well as rainfall intensity and precipitable water content of every radar cell. The contour of the cells could be defined with different reflectivity thresholds. The composite radar picture was generated in every 15th minute. The number and maximum density of flashes, areas, center points are also calculated for flash cells at different density thresholds. Altogether 9 radar cells and 5 flash cells were identified and tracked. The tracked radar cells were defined with 35 dBZ reflectivity threshold, and their main parameters are shown in *Fig. 8*.

Fig. 8. The positions of the tracked radar cells in every 15th minute. The cells are defined with 35 dBZ reflectivity threshold. The main parameters are given: cell ID, mean velocity of motion, direction of motion (also with vectors), maximum reflectivity, and time of observation. The size of a grid is 50×50 km.

The main calculated parameters and features are shown in *Table 3* for radar cells and *Table 4* for flash cells. The cell ID used in figures and tables mark the same thunderstorm cells.

Table 3. Radar characteristics of thunderstorm cells on August 20, 2006

	Maximum reflectivity	**Time**	**Max. area**	**Total water**	**Mean velocity**	**Mean direction**	**Max. area**	**Max. water production**
	dBZ		**km^2**	**million m^3**	**km/h**	**degree**	**km^2**	**million m^3 h^{-1}**
Threshold			**15 dBZ**	**15 dBZ**	**35 dBZ**	**35 dBZ**	**35 dBZ**	**35 dBZ**
Cell ID								
1	57.5	12:45	788	21.9	40.7	86.8	428	13.7
2	58.5	22:15	9062	93.4	96.7	74.3	1404	44.4
3	59.5	18:45	2596	49.0	82.2	85.5	860	24.8
4	58.5	19:45	1153	50.9	78.5	84.3	738	30.1
5	59.5	18:30	805	23.0	62.7	76.9	689	13.6
6	61.5	16:30	759	26.2	50.1	86.0	496	19.0
7	60.5	17:00	532	14.7	32.5	41.2	280	12.2
8	59.5	21:45	2346	46.5	80.3	76.7	810	26.4
9	57.5	23:15	865	27.6	73.8	77.5	349	10.1

Table 4. Lightning characteristics of thunderstorm cells on August 20, 2006

	Max. flash density	**Time**	**Max. area**	**Total flash**	**Mean velocity**	**Mean direction**	**Max. flash area**	**Max. flash activity**
	$km^{-2}\ h^{-1}$		**km^2**		**$km\ h^{-1}$**	**degree**	**km^2**	**h^{-1}**
Threshold			**$2\times km^{-2}\ h^{-1}$**		**$2\times km^{-2}\ h^{-1}$**	**$2\times km^{-2}\ h^{-1}$**	**$2\times km^{-2}\ h^{-1}$**	
Cell ID								
2	28	21:15	1100	5187	96.6	92.4	668	5280
3	15	18:30	354	1313	81.7	86.7	216	1290
4	16	19:45	116	1156	91.6	106.0	64	560
5	12	18:15	176	429	62.0	71.6	76	492

In *Fig. 9* the water and flash production are shown for each tracked convective cells.

Fig. 9. The development of the water production (above) and the flash activity (below) in 15 minutes time intervals for each of tracked thunderstorm cell on August 20, 2006.

In *Table 5* the main radar and lightning characteristics of Budapest storm are summarized.

Table 5. Radar and lightning characteristics of Budapest thunderstorm cells on August 20, 2006

	Radar				**Lightning**			
	Max. dBZ	**Velocity**	**Direction**	**Area**	**Max. flash density**	**Velocity**	**Direction**	**Flash area**
	dBZ	**km h^{-1}**	**degree**	**km^2**	**km^{-2} h^{-1}**	**km h^{-1}**	**degree**	**km^2**
Thres.		**35 dBZ**	**35 dBZ**	**35 dBZ**		**2×km^{-2} h^{-1}**	**2×km^{-2} h^{-1}**	**2×km^{-2} h^{-1}**
Time								
17:00	43.0	0	0	388	6	0	0	60
17:15	50.5	83	82	268	4	172	123	102
17:30	52.5	79	90	538	7	88	85	276
17:45	52.5	86	87	648	4	92	71	196
18:00	53.5	89	75	648	10	144	99	444
18:15	55.5	77	89	780	9	28	146	274
18:30	55.0	74	101	802	15	80	85	354
18:45	59.5	76	84	860	7	64	76	188
19:00	57.0	81	93	598	SAFIR HMS stop			
19:15	46.5	screening		620	10	152	96	188
19:30	50.5	81	33	548	7	80	126	88

On the base of the radar and flash characteristics of tracked cells, the main features of the August 20 storm are the following:

- There was rapid eastward cell displacement this day. The velocity of the cells increased from 40 km/h (cell 1, at noon) to 82 km/h. The direction of motion turned slowly from the east to the north. Most of the thunderstorms involved two or more convective cells.
- The thunderstorm (cell 2) developed in the southeast region of the squall line and produced the maximum number of flashes at 21:15 UTC and precipitable water at 22:15 UTC. The total precipitable water was 94 million m^3, the maximum reflectivity was 58.5 dBZ, and the area of the largest cell was 9000 km^2.
- The most intensive thunderstorm (cell 3) moved almost eastward with a velocity of 82 km/h. The cell reached its maximum phase at 18:45 UTC with maximum reflectivity of 59.5 dBZ. This thunderstorm was composed of different convective cells producing about 49 million m^3 precipitation over a 2500 km^2 area.

- The Budapest storm was initiated by strong convection development at late afternoon in the west Hungary. This development resulted in a rapid gust front moving with about 74–80 km/h to the southeast. The observed reflectivity of the gust front was about 5–10 dBZ. The gust front was observed 1.5 hours ahead by the western radar of the network (Pogányvár C band radar).
- None of the radar cells, that have larger maximum radar reflectivity than 55 dBZ, showed observable flash activities.
- In every cell the flash activity reached its maximum value about 15–45 minutes earlier than the radar reflectivity and precipitable water production reached their maximum values.
- The velocity and the direction of motion of every cell were almost constant, or changed very slowly. This characteristic gave a chance for making forecasts of the cell positions 2–3 hours ahead.

In this research the existence of supercell was investigated by using objective methods. Doppler wind data were applied to find rotating cells using Rankine vortex theory (*Doviak* and *Zrnic*, 1993). The Rankine vortex (RV) model can be applied to recognize mesocyclones with characteristic size of 10 km. Tangential wind component (V_t) of the RV is given by the following equations:

$$V_t(r) = \frac{V_t^{\max}}{R_0} r \qquad \text{if} \quad r \le R_0,$$

$$V_t(r) = \frac{V_t^{\max}}{r} R_0 \qquad \text{if} \quad r > R_0,$$

where r is the distance from the center of RV, R_0 is the "radius" of the vortex, where the tangential wind has its maximum ($V_t^{\max}$).

Rankine vortex theory allows radial inflow or outflow (V_r) of the vortex:

$$V_r(r) = \frac{V_r^{\max}}{R_0} r \quad \text{if} \quad r \le R_0,$$

$$V_r(r) = \frac{V_r^{\max}}{r} R_0 \qquad \text{if} \quad r > R_0,$$

where $V_r^{\max}$ is the maximum radial wind of the vortex at R_0. The vortex could be determined unambiguously, if the coordinates of the center of RV, $V_t^{\max}$ and $V_r^{\max}$, and R_0 were known. For the reason of simplicity, transformation of

radar measured Doppler wind field into storm relative coordinate system is applied. Rankine vortices between diameters of 2 and 10 km were searching in such a way, that all points were tested as a possible center of an RV. A real vortex has to satisfy the following conditions:

(i) Inside the vortex $\frac{\partial V_r}{\partial r} \geq 2.5 \frac{\text{m s}^{-1}}{\text{km}}$.

(ii) $2R_0$ is between 2 and 10 km.

(iii) The explained variance of the tested vortex and the Doppler wind in the storm relative coordinate system has to be higher than 80%.

The most significant RV structures of the Budapest storm were found at 19:11 UTC when Doppler radar scanned at 1° elevation angle (*Fig. 10*). One of the cyclonic rotation center was exactly above the downtown where the Constitution Day firework occurred.

Fig. 10. Doppler wind field in storm relative coordinate system in 30 km radius of Budapest radar on August 20, 2006, 19:11 UTC. Circles show the indicated Rankine vortices with their parameters (ξ: vorticity; R_0: radius of the Rankine vortex; V_{tm}: tangential wind component of the vortex; V_{rm}: radial wind component of the vortex; div: divergence of the vortex). The northern vortex was above the downtown of Budapest.

4. Numerical simulation of the Budapest storm

The aim of the numerical model experiments was to understand the dynamics of thunderstorms like the Budapest storm and to investigate their predictability. The numerical simulations were made by the MM5 Version 3 (NCAR-PSU Mesoscale Model) (*Dudhia*, 1993). The high horizontal resolution (1.5 km) allowed us to run the model without cumulus parameterization. To describe microphysical processes, Reisner microphysical scheme (with five different types of hydrometeors) is applied (*Reisner et al.*, 1998). The planetary boundary layer (PBL) is described by the non-local PBL scheme based on *Troen* and *Mahrt* (1986). Land-surface processes are simulated by the Oregon State University Land-surface Model (*Chen* and *Dudhia*, 2001). For this study, the model was integrated with horizontal resolutions of 1.5 km, with 28 vertical levels on 400 × 500 horizontal grid points. 100 hPa was chosen as the upper level of the model. The model domain was chosen in such a way that the cold front was in the inner part of the model territory at 12:00 UTC initial time. A Lambert-conformal projection was applied with 48.0° latitude and 16.4° longitude central values. An experimental model run with 12 hours forecast needed 4 hours computer time on 64 processors of an ALTX 3700b computer.

The initial and lateral conditions for the MM5 were taken from the ECMWF deterministic model run of 12:00 UTC, on August 20. The ECMWF data set has 0.25 degree resolution. The MM5 model run initiated at 12:00 UTC used the 12:00 UTC ECMWF analysis. The other runs initiated at 13:00 and 14:00 UTC used +1 and +2 hours ECMWF forecast for initial conditions. Input data for MM5 initial condition (mean sea level pressure, three-dimensional temperature, humidity, wind fields, soil temperature and soil humidity values) were taken from the ECMWF analysis.

During model experiments at model run of 14:00 UTC, reflectivity of HMS radar network were also assimilated into initial conditions using the Robust Radar Impact (RRI) method (*Horváth*, 2006). The RRI method is based on theory and numerical experiments which show that the vertical profile of equivalent potential temperature (EPT) can be considered as a nearly constant value, especially in the cases of severe thunderstorms. Supposing that the air in thunderstorms is saturated (relative humidity profile is 100%), it is possible to retrieve a pressure-temperature profile which is valid only in the updraft regions of thunderstorms. In this way thunderstorms appear like warm and wet bubbles isolated from their environment. Case studies were made to determinate the most efficient way to calculate the characteristic EPT value. It was found that EPT of the most unstable layer of the lowest 1000 meters can be considered characteristic for air mass thunderstorms.

A new subprogram which calculates the reflectivity of the precipitation elements (rain, snow, and hail/graupel) was attached to the original code of the MM5. The calculated radar reflectivity field allows us to make a more direct

comparison with the radar observation. (The quantitative comparison between the simulated precipitation intensity and the precipitation intensity derived from the reflectivity is very limited, because the calculation of precipitation field from the radar data bases on crude approximations.) The difficulty of the reflectivity calculation can be handled by supposing that the size of the precipitation elements is small enough to fall into the Rayleigh scattering region, and that the size distributions of these particles are given by an exponential function with fixed intersection parameters. According to *Smith et al*. (1975) the effect of the Mie-theory can be neglected, because the concentration of the hail stones larger than the radar wavelength (3–10 cm) is very small. The dielectric factor of 0.93 and 0.21 were used for the water drops and dry ice particles, respectively. If the temperature is larger than 0°C, the dielectric factor of the ice particles is the same as that of the water drops, because in this case a thin water layer formed on the surface of the ice particles.

3.1 Results of numerical experiments

Several numerical model experiments were made to determinate the optimal model domain and initiation time. A simulation was considered to be successful, if a thunderstorm with mesoscale rotation (mesocyclone) appeared during the simulation. All simulations predicted the cold front passage between 18:00 and 21:00 UTC in Budapest, but severe convective phenomena and associated mesocyclones appeared only in the cases, when at the start of the simulation the cold front was inside the model domain. In cases when the cold front only drifted into the model domain due to the lateral conditions (given by the ECMWF forecast), the model was not able to forecast mesocyclones. In runs with initial times later than 15:00 UTC, the model was not able to develop mesocyclones by 19:00 UTC.

The model run with 12:00 UTC initial time forecasted the squall line and some mesocyclones appeared in the line. However, the dominant supercell moved south of Budapest, and the simulated squall line reached the Danube one hour earlier than in real case. In this case the RRI method was useless, because at the initial time the radar echoes were weak. The most successful model run was when 14:00 UTC initiation was applied. In this case the RRI method helped the model to involve triggers to the appropriate places and passage, and the development of the squall line were closest to reality. Hereafter the results of the 14:00 UTC model run are discussed.

The calculated radar reflectivity seemed to be a good parameter to compare the model simulation with the measured radar data. The model retrieved a realistic image of the real squall line by 15:00 UTC (1 hour forecast), which means that the spin up time was less than one hour. The modeled squall line reached the Austrian-Hungarian border at the same time when the real squall line did. At 17:45 UTC three main calculated reflectivity maxima can be seen in

Fig. 11a. Detailed analysis indicates that all of the three centers had mesocyclone. At this time the southern center had the strongest mesocyclone. At 18:15 UTC already the northern center had the highest reflectivity values and the southern center dropped behind (*Fig. 11b*), while at 18:45 UTC the northern center became obviously the dominant system (*Fig. 11c*). The squall line reached the Danube at 19:15 UTC only 15 minutes later than the real storm did (*Fig. 11d*). A detailed picture of the wind field and the calculated radar echoes show the center of the mesocyclone, which is only a few kilometers from the downtown of Budapest (*Fig. 12*).

Fig. 11. MM5 simulated radar reflectivity (shadowed fields) and 925 hPa wind field of the squall line passage.

Fig. 12. MM5 simulated radar reflectivity and 925 hPa wind field at 19:15 UTC.

The low level thermodynamic characteristics of the squall line are shown by wind and equivalent potential temperature (EPT) fields of the 925 hPa level (*Fig. 13a, b*). The first conspicuous feature is that EPT values rise up behind the leading edge of the squall line. This behavior is opposite to that was found in an earlier investigated supercell occurred in Hungary (*Horváth et al*., 2006). In this case the thunderstorms collected low level unstable air from areas in front of the thunderstorm line, and behind the thunderstorms EPT field formed a cold pool. At the present case the low level pattern of EPT suggests that low level prefrontal instability did not play an important role in supplying of the squall line. Missing of significant cold pools behind the squall line also supports this assumption.

The low level thermodynamic characteristics of the squall line are shown by wind and equivalent potential temperature (EPT) fields of the 925 hPa level (*Fig. 13a, b*). The first conspicuous feature is that EPT values rise up behind the leading edge of the squall line. This behavior is opposite to that was found in an earlier investigated supercell occurred in Hungary (*Horváth et al*., 2006). In this case the thunderstorms collected low level unstable air from areas in front of the thunderstorm line, and behind the thunderstorms EPT field formed a cold pool. At the present case the low level pattern of EPT suggests that low level prefrontal instability did not play an important role in supplying of the squall line. Missing of significant cold pools behind the squall line also supports this assumption.

Fig. 13. MM5 simulated equivalent potential temperature and wind field on the 925 hPa level. Dashed line shows the position of cross-section in Fig. 14.

Fig. 14. Cross-section of MM5 simulated equivalent potential temperature and wind field during the squall line passage. The direction of the squall line is shown in Fig. 13.

Vertical cross sections of the squall line suggest that the unstable air mass which supplied the line of thunderstorms is between 1.5 and 4 km AGL (*Fig. 14a*). This unstable layer is generated by an active wet conveyor belt on the 700 hPa level. (More details about the wet conveyor belt are given at synoptic conditions in Section 2). The cold layer between the 5 and 7 km heights was a

consequence of high level cold advection. This layer was responsible for the prefrontal conditional instability. The cold advection on the 500 hPa level was presented at discussion of the synoptic conditions in Section 2. The squall line can be identified by the towering maximum of EPT up to the troposphere and by lower level directional wind shear (*Fig. 14a, b*). Several parameters were used to analyze the cold front and to separate the front from the squall line. The cross section in *Fig 14b* shows low level cold advection behind the squall line, but there is no significant wind shear (both direction and speed) which would unambiguously indicate the cold front. An option is that the squall line probably blurred the cold front behind itself. The other option is that the squall line accelerated the front, and the separating line between the cold and warm air mass, and the squall line were identical.

5. Conclusion

The Budapest storm was not a classical self propagation squall line, where the cold pool and the low level wind shear play the main role in the formation of line of thunderstorms (*Rotunno*, 1982). The storm can not be place into the certain category of cold front aloft, where high level cold front is responsible for line organized convective storms (*Stoelinga et al.*, 2003). However, the situation was similar to a certain degree.

Basic conditions for convective instability were provided by synoptic scale events and weather patterns. The long frontal system extending across the continent provided good conditions for producing a significant prefrontal wet conveyor belt on the 700 hPa level. This layer supplied convective energy, instead of relative cold and stable lower air, allowing the formation of nocturnal thunderstorms. The frontal wave formed at the southeast Alps caused the air masses to slow down at low level and to run ahead at high level, above the warm sector. Also that wave was responsible for wind shear favorable for supercell formation.

In the unstable prefrontal warm sector a squall line developed and the thunderstorms which hit Budapest were parts of the squall line. The squall line had three main storm centers and by the time of reaching Budapest, the northerly center became the strongest.

Concerning radar reflectivity and lightning activity, the storm and the squall line were not extreme strong events, however, cell motions were very fast. Detailed Doppler wind analysis showed that among cells, which hit Budapest, there were supercells. In spite of the existence of supercells, the typical left or right deviation from the leading squall line direction was not recognized by detailed cell tracking analysis. The extreme fast motion was not favorable for supercell splitting.

High resolution, non-hydrostatic model experiments successfully simulated the squall line and the rotating thunderstorms in time and space. Model results show that thunderstorms got air masses with high equivalent potential temperature from layers between 2–4 km AGL. The air mass near the surface layers were stable, and did not supplied thunderstorms.

The fast moving squall line resulted in that the storm arrived in Budapest about a few hours earlier than the synoptic scale cold front was predicted. Even detailed analysis can not answer obviously, whether the squall line was a prefrontal phenomenon or the cold front became faster because of strong convection, but the direct role of the cold front at the Budapest storm is evident.

***Acknowledgement*—**This research was supported by the NKFP 0022/2005 (Jedlik Ányos) project.

References

Bartha, I., 1987: An objective decision procedure for prediction of maximum wind gusts associated with Cumulonimbus clouds. *Időjárás 91*, 330-346.

Bodolainé, J.E. and *Tänczer, T.*, 2003: *Mesoscale Convective Systems – Triggering Off Flash Floods* (in Hungarian). Országos Meteorológiai Szolgálat, Budapest.

Böjti, B., Bodolainé, J.E., and *Götz, G*., 1964: Instability lines in Hungary (in Hungarian). *Beszámolók az 1964-ben végzett tudományos kutatásokról*. Országos Meteorológiai Szolgálat, Budapest, 139-165.

Chen, F. and *Dudhia, J*.: 2001: Coupling and advanced land surface-hydrology model with the Penn State-NCAR MM5 modeling system. Part I. Model implementation and sensitivity. *Mon. Weather Rev. 129*, 569-585.

Davies-Jones, R., Trapp, R.J., and *Bluestein, H.B.*, 2001: Tornadoes and tornadic storms. In *Severe Convective Storms* (ed.: *C.D. Doswell*). *AMS Meteorological Monographs 28*, No. 50, 167-221.

Doviak, R.J. and *Zrinic, D.S*., 1993: *Doppler Radar and Weather Observations.* Academic Press, 335-340.

Dudhia, J., 1993: A non-hydrostatic version of the Penn State-NCAR Mesoscale Model: Validation tests and simulation of an Atlantic cyclone and cold front. *Mon. Weather Rev*. *121*, 1493-1513.

Fujita, T.T., 1955: Results of detailed synoptic studies of squall lines. *Tellus 7*, 405-436.

Fujita, T.T., 1959: Precipitation and cold air production in mesoscale thunderstorm systems. *J. Meteor. 15*, 454-466.

Geresdi, I. and *Horváth, Á*., 2000: Nowcasting of precipitation type. Part I: Winter precipitation. *Időjárás 104*, 241-252.

Geresdi, I., Horváth, Á., and *Mátyus, Á*., 2004: Nowcasting of the precipitation type Part II: Forecast of thunderstorms and hailstone size. *Időjárás 108*, 33-49.

Götz, G., 1966: *Sturmwarnung am Balatonsee* (in German). Országos Meteorológiai Szolgálat, Budapest.

Götz, G., 1968: Hydrodynamic relationships between heavy convection and the jet stream. *Időjárás 72*, 157-165.

Holton, J.R., 2004: *An Introduction to Dynamic Meteorology*. Elsevier Academic Press.

Horváth, Á.,1997: Tornado (in Hungarian). *Légkör 62,* 2-9.

Horváth, Á., 2006: Numerical studies of severe convective phenomena using robust radar impact method. In *Proceedings of ERAD 2006.* Barcelona, 19-22 September, 557-558.

Horváth, Á. and *Práger, T*., 1985: Study of dynamic and predictability of squall lines (in Hungarian). *Időjárás 89*, 141-160.

Horváth, Á. and *Geresdi, I.*, 2003: Severe storms and nowcasting in the Carpathian Basin. *Atmos. Res. 67-68*, 319-332**.**

Horváth, Á., Geresdi, I., and *Csirmaz, K.*, 2006: Numerical simulation of a tornado producing thunderstorm: A case study. *Időjárás 104*, 279-297.

Hoskins, B.J. and *Bretherton, F.P.*, 1972: Atmospheric frontogenesis models: Matematical formulation and solution. *J. Atmos. Sci. 29*, 11-37.

Houze, R.A., Rutledge, S.A., Biggerstaff, M.I., and *Sull, B.F.*, 1989: Interpretation of Doppler weather radar displays in middle latitude mesoscale convective systems. *B. Am. Meteorol. Soc. 70*, 608-619.

Klemp, J.B. and *Wilhelmson, R.*, 1978: The simulation of three dimensional convective storm dynamics. *J. Atmos. Sci. 35*, 1070-1096.

Klemp, J.B., 1987: Dynamics of tornadic thunderstorms. *Ann. Rev. Fluid Mech. 19*, 369-402.

Lilly, D.K., 1962: On the numerical simulation of buoyant convection. *Tellus XIV*, 148-172.

Reisner, J., Rasmussen, R.M., and *Bruintjes, R.T.*, 1998: Explicit forecasting of supercooled liquid water in winter storms using the MM5 mesoscale model. *Q. J. Roy. Meteor. Soc. 124*, 1071-1107.

Reynolds, D.A. and *Smith, E.*, 1979: Detailed analysis of composited digital radar and satellite data. *B. Am. Meteorol. Soc. 60*, 1024-1037.

Rotunno, R., Klemp, J.B., and *Weisman M.L.*, 1988: A theory for long living squall lines. *J. Atmos. Sci. 45*, 463-485.

Shapiro, M.A., 1982: *Mesoscale Weather Systems of the Central United State*. University of Colorado, Boulder, Co.

Smith, P.L., Jr., Myers, C.G., and *Orville, H.D.*, 1975: Radar reflectivity factor calculations in numerical cloud models using bulk parameterization of precipitation. *J. App. Meteorol. 14*, 1156-1165.

Stoelinga, M.T., Locatelli, J.D., Schwartz, D.R., and *Hobbs, P.V.*, 2003: Is a cold pool necessary for the maintenance of a squall line produced by a cold front aloft? *Mon. Weather Rev. 131*, 95-115.

Troen, I. and *Mahrt, L.*, 1986: A simple model of the atmospheric boundary layer: Sensitivity to surface evaporation. *Bound.-Lay. Meteorol. 37*, 129-148.

Wilhelmson, R.B. and *Wicker, L.J.*, 2001. Numerical modeling of severe local storms. In *Severe Convective Storms* (ed.: *C.D. Doswell*). *AMS Meteorological Monographs 28*, No. 50. 123-166.

Zoltán, Cs. and *Geresdi, I.*, 1984: A one-dimensional steady-state jet model for thunderclouds. *Időjárás 88*, 21-31.